# Synthesis and Application of Three-Dimensional Graphene-Based Aerogels

Subjects: Materials Science, Composites

Contributor: Congling Shi

Aerogel is generated by the replacement of liquid inside a gel with gas by freeze-drying or supercritical drying technique. Three-dimensional graphene-based aerogels (3D GAs), combining the intrinsic properties of graphene and 3D porous structure, can be prepared via self-assembly method, template-guided method and sol-gel process. They have attracted increasing research interest in varied fields with potential applications in photoredox catalysis, biomedicine, energy storage, supercapacitor or other single aspect.

three-dimensional graphene-based aerogels synthetic strategy application

## 1. Introduction

Aerogel, generated by the replacement of liquid inside a gel with gas by freeze-drying or supercritical drying technique, was first presented by S. Kistler in the 1930s [1]. As the lightest solid porous material in the world, it has attracted wide attention owing to its three-dimensional (3D) network structure, high specific surface area, extremely low-density, and thermal conductivity [2][3][4]. The precursor of aerogel can be selected among organic polymers [5], inorganic materials [6], and polymeric hybrid materials [7]. At the beginning, it underwent a long slow-development-stage because of the difficulty in synthesis and the lack of application. However, aerogels with richer types and application fields have been flourishing in the past decade. Such a porous material can be an enticing prospect for its application in the fields of aerospace, chemical engineering, construction, electrical equipment, water purification, and biomedicine [8][9][10][11]. Among them, graphene aerogels [12][13], carbon aerogels [14][15], and carbon nanotube (CNT) aerogels [16] are the most investigated topics, comprising more than 60% of the literature studies.

As the most important component of two-dimensional (2D) carbon-based material, graphene possesses superior thermal conductivity (~5000 W/m·K), high specific surface area (2630 $m^2$/g), chemical stability, and high electron mobility, as well as excellent mechanical and optical properties, which has great application potential in many fields [17]. However, their direct application as excellent adsorbents, anode materials, and mechanical devices suffers from limitation, as a serious loss in surface area occurs due to the re-stacking problem resulting from π-π interaction between graphene layers and the Van der Waals force [18].

The past several years has witnessed explosive interest in constructing a series of composites based on the versatile platform of graphene. In order to overcome the problem and make full use of the characteristics of graphene sheets, the conversion of 2D sheet to 3D porous aerogel via self-assembling by various methods,

including hydrothermal reduction, chemical reduction, crosslinking, and sol-gel processes, is an ideal choice [19]. Due to integration intrinsic properties, including high porosity, conductivity, and feasibility of manufacturing in an industrial scale of graphene and aerogel, 3D GAs have emerged as one of the most exciting and promising materials. The past almost two decades have witnessed a rapid development process in exploring the performance and application of GAs, as reflected in the increasing number of publications collected in the Web of Science database for the search criteria “graphene AND aerogel” (**Figure 1**).

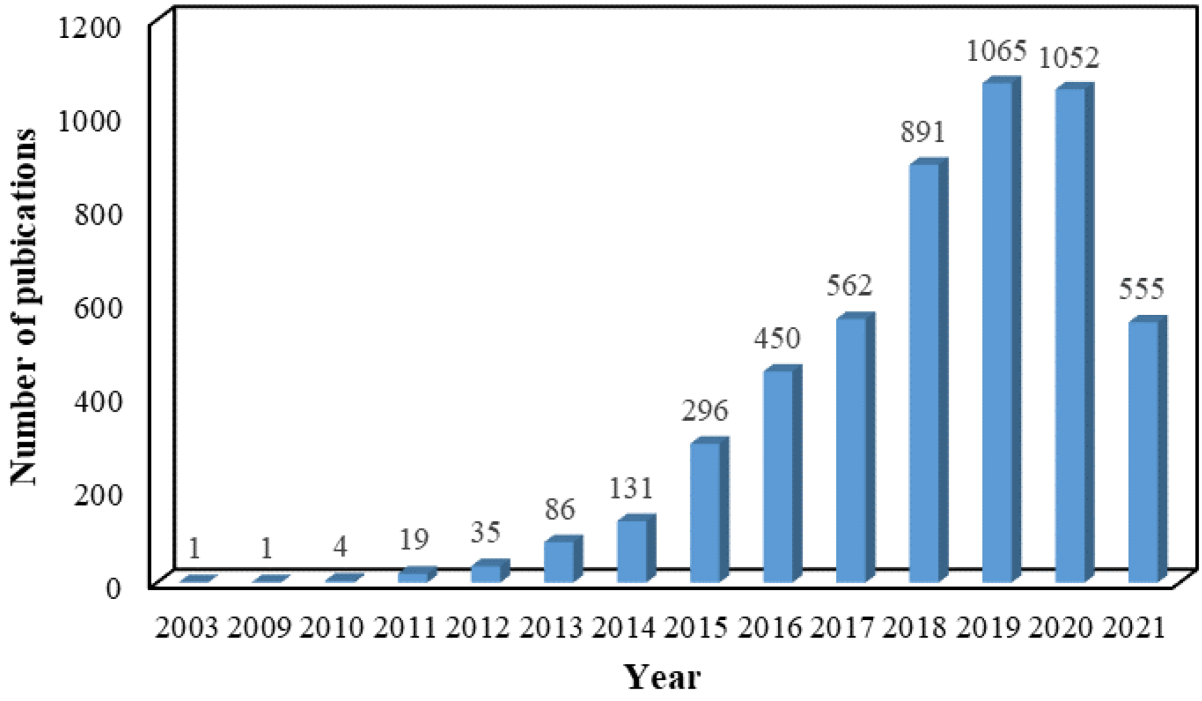


**Figure 1.** Number of publications about GAs in the past almost two decades. Data are summarized on the Web of Science.

## 2. Preparation Strategies

With the further development of 3D GAs, expanded preparation approaches such as hydrothermal reduction [20], chemical reduction [21][22], electrochemical synthesis [23][24], self-assembly [25][26], emulsion technique [27], breath-figure method [28], chemical vapor deposition [29], and ink-printing technique [30] have been adopted to fabricate varied and unique microstructures. Among these, hydrothermal or chemical reduction is the most attractive one based on its low-cost and scalable production.

The interfacial interaction and chemical composition of as-prepared functional GO and/or RGO-based aerogel can be characterized by various means. XPS analysis is performed to characterize both the chemical state and atomic ratio of every element in the GO and the graphene aerogels. For the C 1s XPS spectrum of GA, the peaks attributed to carbon atoms connecting with oxygenated groups, such as C–O and O–C=O, have disappeared as the oxygenated species are substantially removed on the reduction of GO to graphene [31]. It is also evidence for the deoxygenation process and successful preparation of GAs. The significant structural changes are also reflected

in the Raman spectra. The G band, which resonates at a lower frequency and an increased D/G intensity ratio compared to that of GO, suggests a reduction of the exfoliated GO. The FT-IR spectra gives the information of various functional groups, proving the change from graphene oxide into a graphite-like structure due to the chemical reduction.

The graphene-based aerogels are mainly prepared from a GO precursor via the reduction process. The dispersion of graphene in substrate is always particularly important for improving the performance of aerogel. In order to avoid aggregation induced by strong a van der Waals force, many preparation methods involving covalent and/or non-covalent modification between GO and polymer matrix and appropriate ultrasonic dispersion are employed [32]. The dispersion of graphene can be reflected on the morphology of aerogel characterized by SEM, SEM-EDS and TEM, and the XRD pattern. Furthermore, it is feasible to study the dispersion state of graphene by characterizing the typical properties of aerogels based on the obvious effect of dispersion on performance.

### 2.1. Template-Free Approach

A template-free method is preferred in practical application due to the relatively simple synthesis procedures, low cost, and easy scaling up [33]. A series of template-free methods have been put forward for synthesizing 3D GA, in which the most typical and dominant is the self-assembly method. Taking advantage of inherent orderly stacking behavior via π-π interaction of graphene and GO nanosheets under appropriate conditions can produce various 3D structures [34][35][36] without the need and limitation of a template, making it novel and appealing. However, it is still important to develop suitable approaches to achieve the assembly and avoid the precipitation of graphene in a parallel arrangement while declining the repulsion forces of GO solution [37][38][39].

Currently, the widely used methods involve with chemical [40][41][42][43][44][45][46]/hydrothermal [47][48][49][50][51]/electrochemical [52] reduction-induced self-assembly and chemical/physical crosslinking-induced self-assembly [53][54][55][56][57][58][59][60].

### 2.2. Template-Directed Approach

The template-directed strategy, including the emulsion technique, breath figure method, and ink-printing technique, is one of the mainstream approaches employed in the formation of 3D GA with ordered and hierarchical structures [61]. It uses a pre-existing guide (hard or soft template) to directly synthesize the target materials that are difficult to obtain by other tools. Meanwhile, it also inevitably limits the scalability of resulting aerogels owing to the hard accessibility of a well-organized and large-size template itself [62]. The general route for a templated-directed method mainly involves the following steps: (1) template preparation, (2) synthesis of target materials using the template, (3) template removal (if necessary). The obtained aerogels were widely used in lithium-ion batteries and proved to be excellent electrode materials with outstanding performance.

The approach can be classified into hard template method [63][64][65] and soft template method [66][67][68][69].

## 3. Application

Graphene aerogel, with characteristics of low density, high surface area and porosity, and good electrical and thermal conductivity, has attracted the attention of researchers and flourished in the recent decades [70]. They possesses potential application in diverse fields, such as sorption in environmental protection [25][71] electrode materials [72][73], electronic devices [74], flame-retardant and fire-warning materials [75][76], catalysis [77], energy storage [78], and microwave absorption [79].

### 3.1. Aerogels for Absorption

Water contamination caused by harmful chemicals, particularly oils and soluble dyes and phosphate, has become an issue of serious global concern. Various technologies including chemical precipitation [80][81], biological treatment [82], membrane filtration [83][84], adsorption [85], and ion exchange [86] have been employed to remove organic contaminants from wastewater. Among them, the adsorption method has been recognized as the most promising candidate. Therefore, the preparation of novel absorbents with low density, water pickup and cost, high absorption capacity, and good recyclability is in urgent need.

Due to the super-hydrophobicity of GA, it is commonly considered as a competitive and efficient adsorbent for oil in water, with a higher adsorption capacity compared to other kinds of adsorbents [87][88].

### 3.2. Aerogels for Anode Material of Rechargeable Lithium-Ion Batteries

Rechargeable lithium-ion batteries (LIBs) with high energy density and voltage, which can store and supply electricity, have a wide range of applications with the development of modern electronic devices. Currently, the biggest challenge is to develop durable, nontoxic, and inexpensive materials for electrodes.

Owing to the synergetic effect of the super-flexible coating provided by graphene nanosheets and reversible Li+ storage capacity by metal oxide nanoparticles, the composite aerogel has improved performance more suitable for the anode material of LIBs. The high surface area and continuous porous structure of GA is attributed to its superior specific capacitance, making it attractive as advanced electrode materials [89][90][91][92][93][94].

### 3.3. Aerogels with Mechanical Stability for Novel Devices

Two-dimensional graphene/GO with outstanding tensile and compressive strength, high flexibility, and elasticity [95][96] is commonly considered as the most promising building block to fabricate 3D aerogel with mechanical stability. Such an aerogel can be widely employed in flexible electronics, sensors, wearable devices, and smart manufacturing [30]. However, monolithic graphene aerogels formed by random assembly of graphene sheets directly via weak connection often exhibit obvious brittleness in compression as well as stretch [97], and has difficulties meeting the application demands.

There are two main strategies to overcome brittleness to pursue 3D aerogels with mechanical robustness. The predominant approach is to introduce elastic polymers and small molecules acting as cross-linkers or barriers into the matrix [98][99], which is less stable in severe chemical or physical conditions [100]. Another approach is to

enhance the interconnection of aerogels to produce a hierarchical structure by adopting freeze-shaping, 3D ink-printing, and other synergistic assembly techniques [101][102][103].

### 3.4. Aerogels for Fire-Warning Material

The existing commercial fire-warning equipment, including temperature, smoke, and infrared flame detectors, is usually unsatisfactory [104], as they are commonly located at a certain distance from the combustion source and are triggered only when the smoke concentration or temperature reaches a critical value [105]. Consequently, the fire-warning is insensitive, with a response time of more than 100 s [106], which is too late to curb the fire spread and misses the best time for evacuation.

With the increase of temperature, the electrical resistance of GO decreases dramatically, which endows it an attractive application prospect in fire-warning materials [104][107][108]. However, because of its unique porous network structure, aerogel inevitably encounters difficulties in reducing electrical resistance during being burned, which remains a challenge to fabricate sensitive fire-warning aerogels [109][110].

The GO modified aerogel with excellent flame retardancy, thermal isolation, and intrinsic fire warning performance broadens its application territory to cover the drawbacks in delayed response and restricted application scenarios of traditional fire detectors. Therefore, the aerogel that can be triggered in the precombustion stage to offer favorable opportunities for firefighting and emergency rescue is endowed with enticing prospects in chemical industries, pipeline transportation, and high-rise building.

### 3.5. Aerogels for Catalysis

A 3D network structure provides multidimensional electron transport pathways and large accessible surface area, which is conducive to improve the separation efficiency of photogenerated electron-hole pairs and the adsorption of reactants. Such intrinsic hierarchical porous structure characteristics and properties make GAs endowed with potential as promising and efficient photocatalysts for practical applications in solar energy conversion [111], such as pollutant elimination [112], water splitting [113], $CO_2$ reduction [114], and chemical reaction progress [115].

## References

1. Kistler, S.S. Coherent expanded aerogels and jellies. Nature 1931, 127, 741.
2. Yu, M.C.; Zhang, H.M.; Yang, F.L. Hydrophilic and compressible aerogel: A novel draw agent in forward osmosis. ACS Appl. Mater. Inter. 2017, 9, 33948–33955.
3. Antonietti, M.; Fechler, N.; Fellinger, T.-P. Carbon aerogels and monoliths: Control of porosity and nanoarchitecture via sol-gel routes. Chem. Mater. 2013, 26, 196–210.

4. Pierre, A.C.; Pajonk, G.M. Chemistry of aerogels and their applications. Chem. Rev. 2002, 102, 4243–4265.
5. Ulker, Z.; Erkey, C. An emerging platform for drug delivery: Aerogel based systems. J. Control. Release 2014, 177, 51–63.
6. Ziegler, C.; Wolf, A.; Liu, W.; Herrmann, A.K.; Gaponik, N.; Eychmuller, A. Modern Inorganic Aerogels. Angew. Chem. Int. Ed. Engl. 2017, 56, 13200–13221.
7. Liu, Z.J.; Ran, Y.Y.; Xi, J.N.; Wang, J. Polymeric hybrid aerogels and their biomedical applications. Soft Matter 2020, 16, 9160–9175.
8. Stergar, J.; Maver, U. Review of aerogel-based materials in biomedical applications. J. Sol-Gel Sci. Techn. 2016, 77, 738–752.
9. Wang, Y.; Guo, L.; Qi, P.F.; Liu, X.M.; Wei, G. Synthesis of three-dimensional graphene-based hybrid materials for water purification: A review. Nanomaterials 2019, 9, 1123.
10. Xiong, C.Y.; Li, B.B.; Lin, X.; Liu, H.G.; Xu, Y.J.; Mao, J.J.; Duan, C.; Li, T.H.; Ni, Y.H. The recent progress on three-dimensional porous graphene-based hybrid structure for supercapacitor. Compos. Part B Eng. 2019, 165, 10–46.
11. Yan, Z.Q.; Yao, W.L.; Hu, L.; Liu, D.D.; Wang, C.D.; Lee, C.S. Progress in the preparation and application of three-dimensional graphene-based porous nanocomposites. Nanoscale 2015, 7, 5563–5577.
12. Li, G.Y.; Zhang, X.T.; Wang, J.; Fang, J.H. From anisotropic graphene aerogels to electron- and photo-driven phase change composites. J. Mater. Chem. A 2016, 4, 17042–17049.
13. Hu, K.W.; Szkopek, T.; Cerruti, M. Tuning the aggregation of graphene oxide dispersions to synthesize elastic, low density graphene aerogels. J. Mater. Chem. A 2017, 5, 23123–23130.
14. Kim, C.H.J.; Zhao, D.D.; Lee, G.; Liu, J. Strong, machinable carbon aerogels for high performance supercapacitors. Adv. Funct. Mater. 2016, 26, 4976–4983.
15. Lai, F.L.; Miao, Y.-E.; Zuo, L.Z.; Zhang, Y.F.; Liu, T.X. Carbon aerogels derived from bacterial cellulose/polyimide composites as versatile adsorbents and supercapacitor electrodes. Chem. Nano. Mat. 2016, 2, 212–219.
16. Kim, K.H.; Oh, Y.; Islam, M.F. Mechanical and thermal management characteristics of ultrahigh surface area single-walled carbon nanotube aerogels. Adv. Funct. Mater. 2013, 23, 377–383.
17. Korkmaz, S.; Kariper, İ.A. Graphene and graphene oxide based aerogels: Synthesis, characteristics and supercapacitor applications. J. Energy Storage 2020, 27.
18. Dong, Q.C.; Xiao, M.; Chu, Z.Y.; Li, G.C.; Zhang, Y. Recent progress of toxic gas sensors based on 3D graphene frameworks. Sensors 2021, 21, 3386.

19. Franco, P.; Cardea, S.; Tabernero, A.; De Marco, I. Porous aerogels and adsorption of pollutants from water and air: A review. Molecules 2021, 26, 4440.
20. Xu, Y.X.; Sheng, K.X.; Li, C.; Shi, G.Q. Self-assembled graphene hydrogel via a one-step hydrothermal process. ACS Nano 2010, 4, 4324–4330.
21. Zhang, X.T.; Sui, Z.Y.; Xu, B.; Yue, S.F.; Luo, Y.J.; Zhan, W.C.; Liu, B. Mechanically strong and highly conductive graphene aerogel and its use as electrodes for electrochemical power sources. J. Mater. Chem. 2011, 21, 6494–6497.
22. Chen, W.F.; Yan, L.F. In situ self-assembly of mild chemical reduction graphene for three-dimensional architectures. Nanoscale 2011, 3, 3132–3137.
23. Chen, K.W.; Chen, L.B.; Chen, Y.Q.; Bai, H.; Li, L. Three-dimensional porous graphene-based composite materials: Electrochemical synthesis and application. J. Mater. Chem. 2012, 22, 20968–20976.
24. Sheng, K.X.; Sun, Y.Q.; Li, C.; Yuan, W.J.; Shi, G.Q. Ultrahigh-rate supercapacitors based on eletrochemically reduced graphene oxide for ac line-filtering. Sci. Rep. 2012, 2, 247.
25. Cong, H.P.; Ren, X.C.; Wang, P.; Yu, S.H. Macroscopic multifunctional graphene-based hydrogels and aerogels by a metal ion induced self-assembly process. ACS Nano 2012, 6, 2693–2703.
26. He, Y.L.; Li, J.H.; Li, L.F.; Chen, J.B.; Li, J.Y. The synergy reduction and self-assembly of graphene oxide via gamma-ray irradiation in an ethanediamine aqueous solution. Nucl. Sci. Tech. 2016, 27, 61.
27. Huang, X.D.; Sun, B.; Su, D.W.; Zhao, D.Y.; Wang, G.X. Soft-template synthesis of 3D porous graphene foams with tunable architectures for lithium-O2 batteries and oil adsorption applications. J. Mater. Chem. A 2014, 2, 7973–7979.
28. Lee, S.H.; Kim, H.W.; Hwang, J.O.; Lee, W.J.; Kwon, J.; Bielawski, C.W.; Ruoff, R.S.; Kim, S.O. Three-dimensional self-assembly of graphene oxide platelets into mechanically flexible macroporous carbon films. Angew. Chem. Int. Ed. Engl. 2010, 49, 10084–10088.
29. Chen, Z.P.; Ren, W.C.; Gao, L.B.; Liu, B.L.; Pei, S.F.; Cheng, H.M. Three-dimensional flexible and conductive interconnected graphene networks grown by chemical vapour deposition. Nat. Mater. 2011, 10, 424–428.
30. Guo, F.; Jiang, Y.Q.; Xu, Z.; Xiao, Y.H.; Fang, B.; Liu, Y.J.; Gao, W.W.; Zhao, P.; Wang, H.T.; Gao, C. Highly stretchable carbon aerogels. Nat. Commun. 2018, 9, 881.
31. Gong, Y.; Yu, Y.C.; Kang, H.X.; Chen, X.H.; Liu, H.; Zhang, Y.; Sun, Y.M.; Song, H.H. Synthesis and characterization of graphene oxide/chitosan composite aerogels with high mechanical performance. Polymers 2019, 11, 777.

32. Zhuo, B.; Cao, S.A.; Li, X.P.; Liang, J.H.; Bei, Z.H.; Yang, Y.T.; Yuan, Q.P. A nanofibrillated cellulose-based electrothermal aerogel constructed with carbon nanotubes and graphene. Molecules 2020, 25, 3836.
33. Weng, W.S.; Lin, J.; Du, Y.C.; Ge, X.F.; Zhou, X.S.; Bao, J.C. Template-free synthesis of metal oxide hollow micro-/nanospheres via Ostwald ripening for lithium-ion batteries. J. Mater. Chem. A 2018, 6, 10168–10175.
34. Kim, J.; Cote, L.J.; Kim, F.; Yuan, W.; Shull, K.R.; Huang, J. Graphene oxide sheets at interfaces. J. Am. Chem. Soc. 2010, 132, 8180–8186.
35. Li, C.; Shi, G.Q. Three-dimensional graphene architectures. Nanoscale 2012, 4, 5549–5563.
36. Luo, J.; Cote, L.J.; Tung, V.C.; Tan, A.T.; Goins, P.E.; Wu, J.; Huang, J. Graphene oxide nanocolloids. J. Am. Chem. Soc. 2010, 132, 17667–17669.
37. Boukhvalov, D.W.; Katsnelson, M.I. Modeling of graphite oxide. J. Am. Chem. Soc. 2008, 130, 10697–10701.
38. Erickson, K.; Erni, R.; Lee, Z.; Alem, N.; Gannett, W.; Zettl, A. Determination of the local chemical structure of graphene oxide and reduced graphene oxide. Adv. Mater. 2010, 22, 4467–4472.
39. Qin, S.Y.; Liu, X.J.; Zhuo, R.X.; Zhang, X.Z. Microstructure-controllable graphene oxide hydrogel film based on a pH-responsive graphene oxide hydrogel. Macromol. Chem. Phys. 2012, 213, 2044–2051.
40. Chen, W.F.; Yan, L.F. In situ self-assembly of mild chemical reduction graphene for three-dimensional architectures. Nanoscale 2011, 3, 3132–3137.
41. Chen, W.F.; Yan, L.F.; Bangal, P.R. Chemical reduction of graphene oxide to graphene by sulfur-containing compounds. J. Phys. Chem. C 2010, 114, 19885–19890.
42. Zhu, X.J.; Zhu, Y.W.; Murali, S.; Stoller, M.D.; Ruoff, R.S. Nanostructured reduced graphene oxide/Fe2O3 composite as a high-performance anode material for lithium ion batteries. ACS Nano 2011, 5, 3333–3338.
43. Chen, W.F.; Li, S.R.; Chen, C.H.; Yan, L.F. Self-assembly and embedding of nanoparticles by in situ reduced graphene for preparation of a 3D graphene/nanoparticle aerogel. Adv. Mater. 2011, 23, 5679–5683.
44. Li, J.H.; Li, J.Y.; Meng, H.; Xie, S.Y.; Zhang, B.W.; Li, L.F.; Ma, H.J.; Zhang, J.Y.; Yu, M. Ultra-light, compressible and fire-resistant graphene aerogel as a highly efficient and recyclable absorbent for organic liquids. J. Mater. Chem. A 2014, 2.
45. Hu, H.; Zhao, Z.B.; Wan, W.B.; Gogotsi, Y.; Qiu, J.S. Ultralight and highly compressible graphene aerogels. Adv. Mater. 2013, 25, 2219–2223.

46. Sun, H.Y.; Xu, Z.; Gao, C. Multifunctional, ultra-flyweight, synergistically assembled carbon aerogels. Adv. Mater. 2013, 25, 2554–2560.
47. Acik, M.; Lee, G.; Mattevi, C.; Chhowalla, M.; Cho, K.; Chabal, Y.J. Unusual infrared-absorption mechanism in thermally reduced graphene oxide. Nat. Mater. 2010, 9, 840–845.
48. Akhavan, O. The effect of heat treatment on formation of graphene thin films from graphene oxide nanosheets. Carbon 2010, 48, 509–519.
49. Kar, T.; Devivaraprasad, R.; Singh, R.K.; Bera, B.; Neergat, M. Reduction of graphene oxide-a comprehensive electrochemical investigation in alkaline and acidic electrolytes. RSC Adv. 2014, 4, 57781–57790.
50. Liang, J.F.; Liu, Y.K.; Guo, L.; Li, L.D. Facile one-step synthesis of a 3D macroscopic SnO2-graphene aerogel and its application as a superior anode material for Li-ion batteries. RSC Adv. 2013, 3, 11489–11492.
51. Niu, Z.Q.; Liu, L.L.; Zhang, L.; Shao, Q.; Zhou, W.Y.; Chen, X.D.; Xie, S.S. A universal strategy to prepare functional porous graphene hybrid architectures. Adv. Mater. 2014, 26, 3681–3687.
52. Chen, K.W.; Chen, L.B.; Chen, Y.Q.; Bai, H.; Li, L. Three-dimensional porous graphene-based composite materials: Electrochemical synthesis and application. J. Mater. Chem. 2012, 22, 20968–20976.
53. Whitby, R.L. Chemical control of graphene architecture: Tailoring shape and properties. ACS Nano 2014, 8, 9733–9754.
54. Shi, Q.R.; Cha, Y.; Song, Y.; Lee, J.I.; Zhu, C.Z.; Li, X.Y.; Song, M.K.; Du, D.; Lin, Y.H. 3D graphene-based hybrid materials: Synthesis and applications in energy storage and conversion. Nanoscale 2016, 8, 15414–15447.
55. Gao, H.C.; Sun, Y.M.; Zhou, J.J.; Xu, R.; Duan, H.W. Mussel-inspired synthesis of polydopamine-functionalized graphene hydrogel as reusable adsorbents for water purification. ACS Appl. Mater. Inter. 2013, 5, 425–432.
56. Tao, Y.; Kong, D.B.; Zhang, C.; Lv, W.; Wang, M.X.; Li, B.H.; Huang, Z.H.; Kang, F.Y.; Yang, Q.H. Monolithic carbons with spheroidal and hierarchical pores produced by the linkage of functionalized graphene sheets. Carbon 2014, 69, 169–177.
57. Ye, S.B.; Feng, J.C.; Wu, P.Y. Highly elastic graphene oxide-epoxy composite aerogels via simple freeze-drying and subsequent routine curing. J. Mater. Chem. A 2013, 1, 3495–3502.
58. Xu, Y.X.; Wu, Q.; Sun, Y.Q.; Bai, H.; Shi, G.Q. Three-dimensional self-assembly of graphene oxide and DNA into multifunctional hydrogels. ACS Nano 2010, 4, 7358–7362.
59. Qin, Y.; Zhang, Y.; Qi, N.; Wang, Q.Z.; Zhang, X.J.; Li, Y. Preparation of graphene aerogel with high mechanical stability and microwave absorption ability via combining surface support of

metallic-CNTs and interfacial cross-linking by magnetic nanoparticles. ACS Appl. Mater. Inter. 2019, 11, 10409–10417.

60. Arabkhani, P.; Asfaram, A. Development of a novel three-dimensional magnetic polymer aerogel as an efficient adsorbent for malachite green removal. J. Hazard. Mater. 2020, 384, 121394.
61. Liu, Y.D.; Goebl, J.; Yin, Y.D. Templated synthesis of nanostructured materials. Chem. Soc. Rev. 2013, 42, 2610–2653.
62. Sun, H.Y.; Xu, Z.; Gao, C. Multifunctional, ultra-flyweight, synergistically assembled carbon aerogels. Adv. Mater. 2013, 25, 2554–2560.
63. Choi, B.G.; Yang, M.; Hong, W.H.; Choi, J.W.; Huh, Y.S. 3D macroporous graphene frameworks for supercapacitors with high energy and power densities. ACS Nano 2012, 6, 4020–4028.
64. Wang, X.J.; Feng, J.; Bai, Y.C.; Zhang, Q.; Yin, Y.D. Synthesis, properties, and applications of hollow micro-/nanostructures. Chem. Rev. 2016, 116, 10983–11060.
65. Huang, X.D.; Qian, K.; Yang, J.; Zhang, J.; Li, L.; Yu, C.Z.; Zhao, D.Y. Functional nanoporous graphene foams with controlled pore sizes. Adv. Mater. 2012, 24, 4419–4423.
66. Meng, Y.; Gu, D.; Zhang, F.Q.; Shi, Y.F.; Yang, H.F.; Li, Z.; Yu, C.Z.; Tu, B.; Zhao, D.Y. Ordered mesoporous polymers and homologous carbon frameworks: Amphiphilic surfactant templating and direct transformation. Angew. Chem. Int. Ed. Engl. 2005, 44, 7053–7059.
67. Lu, K.Q.; Xin, X.; Zhang, N.; Tang, Z.R.; Xu, Y.J. Photoredox catalysis over graphene aerogel-supported composites. J. Mater. Chem. A 2018, 6, 4590–4604.
68. Yin, S.Y.; Zhang, Y.Y.; Kong, J.H.; Zou, C.J.; Li, C.M.; Lu, X.H.; Ma, J.; Boey, F.Y.; Chen, X.D. Assembly of graphene sheets into hierarchical structures for high-performance energy storage. ACS Nano 2011, 5, 3831–3838.
69. Hou, X.F.; Zheng, Y.H.; Ma, X.L.; Liu, Y.H.; Ma, Z.C. The effects of hydrophobicity and textural properties on hexamethyldisiloxane adsorption in reduced graphene oxide aerogels. Molecules 2021, 26, 1130.
70. Sui, Z.Y.; Meng, Y.N.; Xiao, P.W.; Zhao, Z.Q.; Wei, Z.X.; Han, B.H. Nitrogen-doped graphene aerogels as efficient supercapacitor electrodes and gas adsorbents. ACS Appl. Mater. Inter. 2015, 7, 1431–1438.
71. Hu, H.; Zhao, Z.B.; Gogotsi, Y.; Qiu, J.S. Compressible carbon nanotube-graphene hybrid aerogels with superhydrophobicity and superoleophilicity for oil sorption. Environ. Sci. Tech. Let. 2014, 1, 214–220.
72. Wang, J.; Fang, F.; Yuan, T.; Yang, J.H.; Chen, L.; Yao, C.; Zheng, S.Y.; Sun, D.L. Three-dimensional graphene/single-walled carbon nanotube aerogel anchored with SnO2 nanoparticles for high performance lithium storage. ACS Appl. Mater. Inter. 2017, 9, 3544–3553.

73. Wu, Z.S.; Yang, S.B.; Sun, Y.; Parvez, K.; Feng, X.L.; Mullen, K. 3D nitrogen-doped graphene aerogel-supported Fe3O4 nanoparticles as efficient electrocatalysts for the oxygen reduction reaction. J. Am. Chem. Soc. 2012, 134, 9082–9085.
74. Hu, Y.J.; Zhuo, H.; Chen, Z.H.; Wu, K.Z.; Luo, Q.S.; Liu, Q.Z.; Jing, S.S.; Liu, C.F.; Zhong, L.X.; Sun, R.C.; et al. Superelastic carbon aerogel with ultrahigh and wide-range linear sensitivity. ACS Appl. Mater. Inter. 2018, 10, 40641–40650.
75. Cao, C.R.; Yuan, B.H. Thermally induced fire early warning aerogel with efficient thermal isolation and flame-retardant properties. Polym. Advan. Technol. 2021, 32, 2159–2168.
76. Zuo, B.Y.; Yuan, B.H. Flame-retardant cellulose nanofiber aerogel modified with graphene oxide and sodium montmorillonite and its fire-alarm application. Polym. Advan. Technol. 2021, 32, 1877–1887.
77. Tong, Z.W.; Yang, D.; Shi, J.F.; Nan, Y.H.; Sun, Y.Y.; Jiang, Z.Y. Three-dimensional porous aerogel constructed by g-C3N4 and graphene oxide nanosheets with excellent visible-light photocatalytic performance. ACS Appl. Mater. Inter. 2015, 7, 25693–25701.
78. Ren, L.; Hui, K.N.; Hui, K.S.; Liu, Y.D.; Qi, X.; Zhong, J.X.; Du, Y.; Yang, J.P. Corrigendum: 3D hierarchical porous graphene aerogel with tunable meso-pores on graphene nanosheets for high-performance energy storage. Sci. Rep. 2016, 6, 17243.
79. Qin, Y.; Zhang, Y.; Qi, N.; Wang, Q.Z.; Zhang, X.J.; Li, Y. Preparation of graphene aerogel with high mechanical stability and microwave absorption ability via combining surface support of metallic-CNTs and interfacial cross-linking by magnetic nanoparticles. ACS Appl. Mater. Inter. 2019, 11, 10409–10417.
80. Chen, Q.Y.; Luo, Z.; Hills, C.; Xue, G.; Tyrer, M. Precipitation of heavy metals from wastewater using simulated flue gas: Sequent additions of fly ash, lime and carbon dioxide. Water. Res. 2009, 43, 2605–2614.
81. Chen, Q.Y.; Yao, Y.; Li, X.Y.; Lu, J.; Zhou, J.; Huang, Z.L. Comparison of heavy metal removals from aqueous solutions by chemical precipitation and characteristics of precipitates. J. Water Process Eng. 2018, 26, 289–300.
82. Tsai, W.T.; Chen, H.R. Removal of malachite green from aqueous solution using low-cost chlorella-based biomass. J. Hazard. Mater. 2010, 175, 844–849.
83. Doke, S.M.; Yadav, G.D. Novelties of combustion synthesized titania ultrafiltration membrane in efficient removal of methylene blue dye from aqueous effluent. Chemosphere 2014, 117, 760–765.
84. Leo, C.P.; Chai, W.K.; Mohammad, A.W.; Qi, Y.; Hoedley, A.F.; Chai, S.P. Phosphorus removal using nanofiltration membranes. Water. Sci. Technol. 2011, 64, 199–205.

85. Akhurst, D.J.; Jones, G.B.; Clark, M.; McConchie, D. Phosphate removal from aqueous solutions using neutralised bauxite refinery residues (Bauxsol™). Environ. Chem. 2006, 3, 65–74.
86. Terry, T.A. Removal of nitrates and phosphates by ion exchange with hydrotalcite. Environ. Eng. Sci. 2009, 26, 691–696.
87. Nguyen, D.D.; Tai, N.H.; Lee, S.B.; Kuo, W.S. Superhydrophobic and superoleophilic properties of graphene-based sponges fabricated using a facile dip coating method. Energy Environ. Sci. 2012, 5, 7908–7912.
88. Tran, D.N.H.; Kabiri, S.; Wang, L.; Losic, D. Engineered graphene-nanoparticle aerogel composites for efficient removal of phosphate from water. J. Mater. Chem. A 2015, 3, 6844–6852.
89. Gomez-Navarro, C.; Weitz, R.T.; Bittner, A.M.; Scolari, M.; Mews, A.; Burghard, M.; Kern, K. Electronic transport properties of individual chemically reduced graphene oxide sheets. Nano. Lett. 2007, 7, 3499–3503.
90. Wang, H.L.; Cui, L.F.; Yang, Y.; Sanchez Casalongue, H.; Robinson, J.T.; Liang, Y.Y.; Cui, Y.; Dai, H.J. Mn3O4-graphene hybrid as a high-capacity anode material for lithium ion batteries. J. Am. Chem. Soc. 2010, 132, 13978–13980.
91. Zhou, G.M.; Wang, D.W.; Li, F.; Zhang, L.L.; Li, N.; Wu, Z.S.; Wen, L.; Lu, G.Q.; Cheng, H.M. Graphene-wrapped Fe3O4 anode material with improved reversible capacity and cyclic stability for lithium ion batteries. Chem. Mater. 2010, 22, 5306–5313.
92. Ji, L.W.; Tan, Z.K.; Kuykendall, T.R.; Aloni, S.; Xun, S.D.; Lin, E.; Battaglia, V.; Zhang, Y.G. Fe3O4 nanoparticle-integrated graphene sheets for high-performance half and full lithium ion cells. Phys. Chem. Chem. Phys. 2011, 13, 7170–7177.
93. Askari, M.B.; Salarizadeh, P.; Seifi, M.; Ramezan zadeh, M.H.; Di Bartolomeo, A. ZnFe2O4 nanorods on reduced graphene oxide as advanced supercapacitor electrodes. J. Alloys Compd. 2021, 860, 158497.
94. Zhang, M.; Lei, D.N.; Yin, X.M.; Chen, L.B.; Li, Q.H.; Wang, Y.G.; Wang, T.H. Magnetite/graphene composites: Microwave irradiation synthesis and enhanced cycling and rate performances for lithium ion batteries. J. Mater. Chem. 2010, 20.
95. Dikin, D.A.; Stankovich, S.; Zimney, E.J.; Piner, R.D.; Dommett, G.H.; Evmenenko, G.; Nguyen, S.T.; Ruoff, R.S. Preparation and characterization of graphene oxide paper. Nature 2007, 448, 457–460.
96. Kim, K.H.; Oh, Y.; Islam, M.F. Graphene coating makes carbon nanotube aerogels superelastic and resistant to fatigue. Nat. Nano-Technol. 2012, 7, 562–566.
97. Qiu, L.; Liu, J.Z.; Chang, S.L.; Wu, Y.Z.; Li, D. Biomimetic superelastic graphene-based cellular monoliths. Nat. Commun. 2012, 3, 1241.

98. Yilmaz, G.; Lu, X.M.; Ho, G.W. Cross-linker mediated formation of sulfur-functionalized V2O5/graphene aerogels and their enhanced pseudocapacitive performance. Nanoscale 2017, 9, 802–811.
99. Lee, B.; Lee, S.; Lee, M.; Jeong, D.H.; Baek, Y.; Yoon, J.; Kim, Y.H. Carbon nanotube-bonded graphene hybrid aerogels and their application to water purification. Nanoscale 2015, 7, 6782–6789.
100. Tang, Y.; Gong, S.; Chen, Y.; Yap, L.W.; Cheng, W.L. Manufacturable conducting rubber ambers and stretchable conductors from copper nanowire aerogel monoliths. ACS Nano 2014, 8, 5707–5714.
101. Si, Y.; Yu, J.Y.; Tang, X.M.; Ge, J.L.; Ding, B. Ultralight nanofibre-assembled cellular aerogels with superelasticity and multifunctionality. Nat. Commun. 2014, 5, 5802.
102. Qi, H.S.; Mäder, E.; Liu, J.W. Electrically conductive aerogels composed of cellulose and carbon nanotubes. J. Mater. Chem. A 2013, 1, 9714–9720.
103. Fratzl, P.; Weinkamer, R. Nature’s hierarchical materials. Prog. Mater. Sci. 2007, 52, 1263–1334.
104. Xie, H.L.; Lai, X.J.; Li, H.Q.; Gao, J.F.; Zeng, X.R.; Huang, X.Y.; Lin, X.Y. A highly efficient flame retardant nacre-inspired nanocoating with ultrasensitive fire-warning and self-healing capabilities. Chem. Eng. J. 2019, 369, 8–17.
105. Evans, D.D.; Stroup, D.W. Methods to calculate the response time of heat and smoke detectors installed below large unobstructed ceilings. Fire Technol. 1986, 22, 54–65.
106. Qualey Iii, J.R. Fire test comparisons of smoke detector response times. Fire Technol. 2000, 36, 89–108.
107. Xie, H.L.; Lai, X.J.; Li, H.Q.; Gao, J.F.; Zeng, X.R.; Huang, X.Y.; Zhang, S.F. A sandwich-like flame retardant nanocoating for supersensitive fire-warning. Chem. Eng. J. 2020, 382, 122929.
108. Chen, J.Y.; Xie, H.L.; Lai, X.J.; Li, H.Q.; Gao, J.F.; Zeng, X.R. An ultrasensitive fire-warning chitosan/montmorillonite/carbon nanotube composite aerogel with high fire-resistance. Chem. Eng. J. 2020, 399, 125729.
109. Chen, Z.H.; Hu, Y.J.; Zhuo, H.; Liu, L.X.; Jing, S.S.; Zhong, L.X.; Peng, X.W.; Sun, R.C. Compressible, elastic, and pressure-sensitive carbon aerogels derived from 2D titanium carbide nanosheets and bacterial cellulose for wearable sensors. Chem. Mater. 2019, 31, 3301–3312.
110. Pang, Y.; Zhang, K.N.; Yang, Z.; Jiang, S.; Ju, Z.Y.; Li, Y.X.; Wang, X.F.; Wang, D.Y.; Jian, M.Q.; Zhang, Y.Y.; et al. Epidermis microstructure inspired graphene pressure sensor with random distributed spinosum for high sensitivity and large linearity. ACS Nano 2018, 12, 2346–2354.
111. Zhang, N.; Yang, M.Q.; Liu, S.Q.; Sun, Y.G.; Xu, Y.J. Waltzing with the versatile platform of graphene to synthesize composite photocatalysts. Chem. Rev. 2015, 115, 10307–10377.

112. Wan, W.C.; Yu, S.; Dong, F.; Zhang, Q.; Zhou, Y. Efficient C3N4/graphene oxide macroscopic aerogel visible-light photocatalyst. J. Mater. Chem. A 2016, 4, 7823–7829.
113. Park, J.; Jin, T.; Liu, C.; Li, G.H.; Yan, M.D. Three-dimensional graphene-TiO2 nanocomposite photocatalyst synthesized by covalent attachment. ACS Omega 2016, 1, 351–356.
114. Yang, M.Q.; Zhang, N.; Wang, Y.; Xu, Y.J. Metal-free, robust, and regenerable 3D graphene-organics aerogel with high and stable photosensitization efficiency. J. Catal. 2017, 346, 21–29.
115. Gao, M.M.; Peh, C.K.N.; Ong, W.L.; Ho, G.W. Green chemistry synthesis of a nanocomposite graphene hydrogel with three-dimensional nano-mesopores for photocatalytic H2 production. RSC Adv. 2013, 3, 13169–13177.